Mem. Natl Inst. Polar Res., Spec. Issue, **49**, 281–290, 1994

CONTINUOUS STUDY OF AN ICE CORE: ECM, FINE STRATIGRAPHY, AIR BUBBLES AND CRYSTALS

V. ZAGORODNOV[1], J. J. KELLEY[1], L. THOMPSON[2]
and Okitsugu WATANABE[3]

[1]*Polar Ice Coring Office, University of Alaska Fairbanks, Fairbanks, Alaska 99775-1710, U. S. A.*
[2]*Byrd Polar Center, Ohio State University, Columbus, U. S. A.*
[3]*National Institute of Polar Research, 9-10, Kaga 1-chome, Itabashi-ku, Tokyo 173*

Abstract: The continuous multi-parameter analysis of an ice core reduces time required for field and laboratory investigations. A method for producing a continuous thin section (TS) along an ice core is described. Semiconductor laser sensors (LS) and multiple electrodes were used for continuous measurements of electrical and optical parameters of the TS along the ice core. An ice core volume of 3–5% is thrown out during ice core preparation for Electrical Conductivity Measurements (ECM), stratigraphy, air bubbles concentration, average bubble diameter, and linear dimensions of ice crystals.

A modified commercial LS has a spatial resolution about 0.1 mm. Opaque objects, about 1 μm diameter, can be detected inside a TS. The concentration and average diameter of air bubbles can be measured. The fine stratigraphy of an ice core caused by air bubbles or solid particles can be studied inside a TS by LS. Using polarization effects, linear dimensions of ice crystals can be measured.

1. Introduction

Beginning in the late seventies, continuous methods of ice core analysis were developed (HAMMER *et al.*, 1978; HAMMER, 1980; STAUFFER *et al.*, 1989; ZAGORODNOV and ARKHIPOV, 1990; ZAGORODNOV *et al.*, 1991; TAYLOR *et al.*, 1992). Continuous study of ice cores using an Ice Core Analytical System (ICAS) has several advantages:

1) continuous profiles can be obtained;
2) data processing speed is increased; and
3) only a small portion of an ice core is wasted.

During laboratory investigations of a single parameter of an ice core 90% of the total time required for core retrieval, unpacking, fitting and repacking (HAMMER *et al.*, 1985). Obviously, multi-parameter ice core study will save routine work time.

There are several types of Electrical Conductivity Measurements (ECM) apparatus described in the literature (HAMMER, 1980; DANSGAARD *et al.*, 1985; SCHWANDER *et al.*, 1983). The latest modification of the ECM method involved application of a high voltage (2500 V) and a relatively high speed electrode motion (80–100 mm/s). This allowed a reduction in the signal to noise ratio (TAYLOR *et al.*, 1992). Spatial resolution of the ECM method was estimated as 2 mm (HAMMER, 1980). Currently, the (ECM) method is most common for detection of acidity and annual layers of an ice core. Using a rail system for carrying instruments along an ice core allows continuous measurement of different parameters. Modification of the ECM method using alternating current offers the possibility of measuring ion composition of an ice core. The intensity of gamma-rays passing through the ice depends on their density. Measurements of gamma-ray absorption along an ice core allows for the obtaining the continuous profile of ice core density. Ice crystals and air bubbles detection were performed using an automated device (ZAGORODNOV *et al.*, 1991).

To obtain detailed information on climate and environmental history it is often necessary to analyze thin (less then 1 mm) metamorphosed ice layers in an ice core. Both electrical and optical properties of ice can be measured continuously along the ice core. The major advantages of optical sensing are: no-contact measurements and the possibility of using both wide and narrow light beams. Experiments with natural ice cores obtained at Mizuho Station (Antarctica) and Greenland Summit were carried out in the cold laboratories of the National Institute of Polar Research (NIPR) (Japan) and the Byrd Polar Research Center, Ohio State University (U. S. A.). A continuous thin section formatting procedure was tested at the GISP2 drilling site. The goal of the experiments presented below was to develop methods of the multi-parameter continuous analysis of an ice core primarily for the study of thin (a few millimeters) annual stratigraphy. Some electrical (1000 VDC) and optical (wave length 780 nm) properties of the ice cores were investigated.

2. Ice Core Analytical System (ICAS)

The general schematic of the apparatus for multi-parameter continuous ice core investigations—Ice Core Analytical System (ICAS)—is shown in Fig. 1. ICAS consists of a carriage holding a segment of an ice core which moves along rails, cutting tools, array of sensors, data acquisition and control panel. A portable system was developed for field and laboratory study of short (<0.4 m) segments of ice core. Analyzing procedures include formatting thin section along an ice core segment and longitudinal measurements of its electrical and optical parameters along the same route.

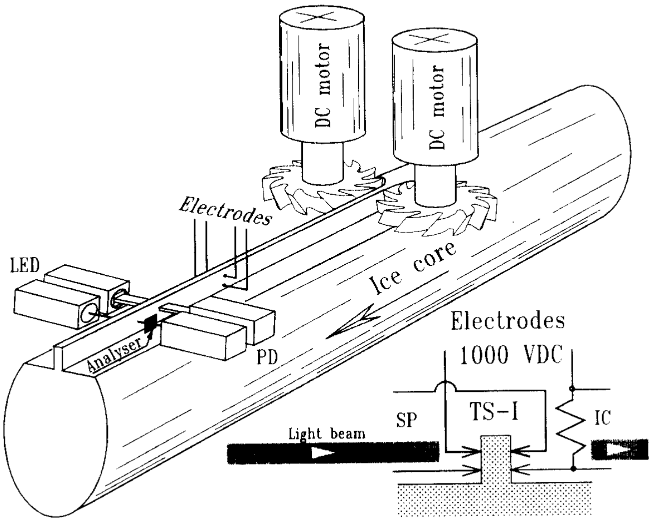

Fig. 1. Schematic of the Ice Core Analytical System: SP–surface potential output, IC–initial current (ECM) output, ED–light-emitting diodes, PD–photo diodes.

2.1. *Thin section formatting*

Cylindrical (half or quarter) segments of an ice core have been fixed on the carriage and moved along the rails (Fig. 2). A synchronous AC motor (4 W) with reducer provides constant speed motion of the core segment through thin section formatting instruments and sensor arrays. The dimensions of the ice core segments and TS in Fig. 2 were taken from successful experiments. Thin section formation and optical measurements were done at the speed of 2.6 mm/s, and electrical measurements took place at 30 mm/s. The thin section-I (TS-I) (Fig.1) was formatted during cutting by two mills (OD 80 mm) mounted on shafts of two DC motors (7.000–10.000 rpm; 150 W). To create a very thin (0.15 mm) section-II (TS-II), felt disks were used rather than mills. High speed DC motors (8.000–12.000 rpm; 4 W) were used for the operation. Maximum tested speed of the TS-I and TS-II formation was 6 mm/s (about 21.5 m/hr). The thin sections (TS-I and TS-II) made from fresh Greenland ice core, recovered from a depth about 120 m, did not contained visible cracks. Only 3 to 5% of the ice core volume is wasted for a 10-mm height TS. In different experiments TS-I had thicknesses of d=4.5 and 6 mm and was used for the study of electrical and optical properties. TS-II with d=0.15 mm was used for measurements of linear dimensions of ice crystals. Measurements of the TS thickness have been done using micrometer with 0.01-mm resolution. Both cross-sectional and longitudinal variations of the thickness of TS-I did not exceed 0.1 mm. A visual inspection of the TS-II showed that thickness increases from approximately 0.5 mm at the base to the 0.1 mm or less at the top. Longitudinal TS-II thickness variations do not exceed 0.1 mm. For precise TS thickness measurements, special optical devices should be used.

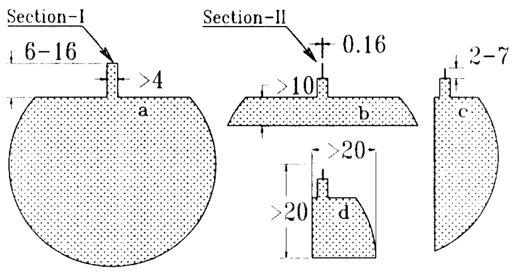

Fig. 2. Versions of thin sections formatting; dimensions in mm.

Results of the TS investigations presented below were obtained using various rail systems with different positioning mechanisms for cutting instruments and sensors. But processing tools, as well as sensors, have not been significantly changed. Thus, the quality of the TS-I and TS-II used in the different experiments was similar and the results obtained were comparable.

2.2. *Electrodes*

The current between two electrodes with applied DC voltage moving over a surface of an ice core is the initial current (IC) in the buildup of space charges (HAMMER, 1980, 1983). Evidently, if the electrodes touch the opposite sides of the thin section, a similar electrical phenomenon will occur. The TS shape and size are parameters which determine the number of the charges and parameters of the electric field between the electrodes. If the thickness of the TS is constant, then initial current depend on the concentration of the impurity in the ice. The deference of potential between two electrodes placed in electric field of the current electrodes depends on IC and parameters of the substance between electrodes. To prove these assumptions, multiple electrodes for measure of initial current and surface potential (SP) were designed (Fig. 1). Two pair of V-shape spring (0.3 mm diameter wire) electrodes touch the TS-I from opposite sides. The contact area of each electrode is approximately 0.25 mm^2. The TS fits loosely through the electrodes in both directions. The vertical distance between the electrodes was 2 mm, and the horizontal distance depended on the thickness of the thin sections. In this way, measurement of initial current are similar to the ECM method. The IC and the SP were measured during different runs. The time between runs was 0.5–5 min. Electrical measurements were conducted using 1000 VDC applied potential. The described electrodes allowed us to measure electrical parameters of an ice core on the same route as optical sensing. Registration of initial current and surface potential, as well as optical sensors output, was accomplished by a single channel chart recorder. Electrical and optical measurements were conducted at temperatures of –8 ~ –9°C.

2.3. Optical sensors

Optical measurements were done by commercial laser photoelectric sensors (LS) (Keyence Corp.). LS consist of a semiconductor laser light source and a photo receiver situated on a straight line. When an object is passing through the laser light beam, between the light source (780 nm wavelength; 3 mW) and the receiver, it causes a change in the light quantity. The intensity of the beam passing through an empty space between the light source and the receiver was used as a 100% (maximum output 5.1 V) reference. The output signal is proportional to the interrupted area of the laser beam. Modifications of the LS allow us to obtain plane polarized monochromatic light beams: rectangular (2×4 mm) and elliptical (0.1 mm) form in focal plane (Fig. 1). The detection limit of the sensor in focal plane of the narrow beam was 1 μm diameter for a single opaque object. The broad beam limit was about a 100 μm diameter object. Resolution of photo diodes in 5.1 V full output range (advanced sensor) was 4 mV. Optical sensors have been tested within the temperature range of –62 to +50°C and have performed with stable characteristics.

Two types of the longitudinal optical measurements were done: (1) the variations of the intensity of the wide light beam passed through the TS-I or optical density (OD) and (2) the intensity of the narrow beam passed trough TS-II and analyzer. The latter measurements were conducted at various incidence angles of the light beam relative to the TS-II plane. In Fig. 1 the light beam polarization plane is vertical. The plane of the scanning was perpendicular to TS-II and the polarization plane was perpendicular to the scanning plane. Both the electrical and the optical measurements have been done along the same track.

3. Experiments

3.1. Initial current and surface potential of an ice core

Results of IC and SP measurements at a speed of 30 mm/s are shown in Fig. 3. When the electrical measurements have been done at speed of 2.6 mm/s the output signals on IC resistor (8.2 kΩ) do not exceed the apparatus noise (0.1 mV). Profiles marked *d*=6 mm and *d*=4.5 mm were obtained at 8 and 20 mm, respectively, below the ice core surface.

According to Hammer's description of the ECM method, the IC has a maximum value during the first 0.1–0.5 s when the electrodes touch the ice surface (HAMMER, 1980). Then the current decreases exponentially. Hence, small values of the initial current at low speed can be explained by finishing buildup of the space charges. It follows that, in the case of the thin section ECM measurements, the same mechanism of the buildup of space charges takes place. Because surface potential arises only during high speed electrode events, this parameter may also represent the buildup of space charges.

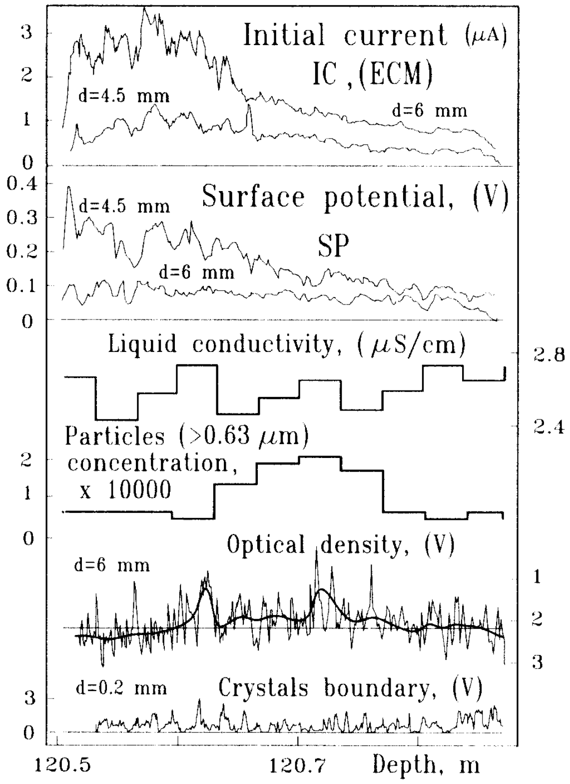

Fig. 3. Parameters of the Greenland Summit ice core; #5, 1989.

The effect of a TS thickness was determined when electrical measurements along the same segment of an ice core were conducted at *d*=6 and 4.5 mm. At high speed, values of the IC was approximately 3 times higher when *d*=6 mm compared to *d*=4.5 mm. On the contrary, the SP increases in the same proportion when TS thickness decreases from 6 to 4.5 mm. Both pair of IC and SP profiles demonstrate similar general trends and features. Results of repeated measurements (0.5–5 min) showed very small variation of the amplitude and position of the IC and SP features. Base on liquid conductivity and particle concentration profiles the thickness of annual layers in this segment of the ice core are close to 0.3 m. Presumably, IC and SP profiles in Fig. 3 represent a one-year accumulation layer.

3.2. Optical density and stratigraphy

Part of the energy that falls on ice is reflected from the surface. According to HOBBS (1974), when visible light falls normally to air-ice or ice-air interface, the amount of reflected energy is 1.8% of incident energy. The absorption coefficient of clear ice at 780 nm wavelengths is about 0.015 cm^{-1} (HOBBS, 1974). In the case of transmitting light through the 0.2 and 6 mm thick, clear ice plates, absorption is equal to 0.03 and 0.9% of incident energy, respectively. Thus, variations of the intensity of the light passed through the TS (d=6±0.1 mm) of clear ice caused by changing TS thickness should not exceed 4 mV. A clear, polycrystalline ice, composed of crystals of average diameter 1 mm, absorbs the same quantity of light as a single crystal of ice (HOBBS, 1974). Hence, light reflection from the TS surface and absorption by clear ice are negligible.

The absorption coefficient of bubbly ice is larger due to scattering from the air bubbles (HOBBS, 1974; LANE, 1975). Approximately 40–60% of energy passes through the bubbly lake or artificial ice. Numerous investigations show that the density of glacier ice depends on the volume of air bubbles (BUTKOVICH, 1953; SHUMSKII, 1955; LANGWAY, 1958; GOW, 1963). As a first approximation, density of glacier ice (ρg) can be described by NAKAWO and NARITA (1985): $\rho g=\rho_i[1-4/3(\pi r^3 n)]$, where ρ_i is the density of pure ice, r and n are the radius and the concentration of air bubbles, respectively. Experimental data (BARKOV and LIPENKOV, 1984; NARITA and NAKAWO, 1985) show that in antarctic ice n varied between 0.2 and 0.8 mm^{-3} and r from 0.1 to 1.0 mm. If bubbles are dispersed uniformly in an ice core, then one bubble would occupy from 1.25 to 5 mm^3. Narrow (0.1 mm) light beam passing through 6 mm thick TS-I (Fig. 1) interacts with V_i=0.06 mm^3 volume of ice. If TS-I has a thickness of 2 mm, then V_i=0.02 mm^3. Hence, the narrow beam allows us to measure the magnitude of n. The broad beam passing through TS-I (6 mm) and interacts with V_i=48 mm. In the latter case, intensity of the light passing through TS-I depends on n and on the radius of air inclusions. When n is known, it is possible to calculate r. Dimensions of the TS and the light beams can by adjusted to specific parameters of air inclusions.

In order to determine true density from the optical data, several effects should be investigated: (1) temperature (BUTKOVICH, 1953), (2) bubbles' size distribution (BARKOV and LIPENKOV, 1984), (3) surface factor (HIGASHI *et al.*, 1983; NAKAWO and NARITA, 1985), (4) ice relaxation (LANGWAY, 1958; SHOJI and LANGWAY, 1983), (5) insoluble inclusions, and micro-fractures (NAKAWO and NARITA, 1985).

The density of glacier ice is subjected to seasonal variations (LANGWAY, 1967; SHOJI and LANGWAY, 1989). At the pore close-off level, the density variations are about 10–50 kg/m^3. Melt features increase this variation (BENSON, 1959). The use of ICAS seasonal optical density variations have been found in Greenland Summit ice core. The optical density profile in Fig. 3 has a darker fragment which correlates with the spring/summer peak of microparticles concentration. High frequency noise on the optical density (OD) profile appear due to not uniform bubbles distribution. Short-term OD variations presumably correspond to wind and radiation crusts. Based on presented results, one may assume that the described optical sensor (broad beam) allows for the detection of 1–2-mm thick stratigraphy features. The resolution of the above method can be increased by application of a narrow beam sensor.

3.3. Ice crystals linear dimensions

The intensity of a plane-polarized light beam passing through a single ice crystal and analyzer depends on the orientation of the crystal optic axes. Therefore, the intensity will change abruptly as the light beam moves from one crystal to another. Two parallel, vertical sections of the Mizuho ice core were fabricated (ZAGORODNOV *et al.*, 1991). The first section (Fig. 4a) was prepared by band saw and microtome shaving; the second (Fig. 4b), by ICAS. Longitudinal scanning profiles of the TS-II taken by laser sensors are shown in Fig. 4. Both profiles demonstrate an abrupt change of light intensity when the light beam crosses the grain boundaries detected on the photographs. The thicker section (Fig. 4b) demonstrates a maximal variation of the output signal of 5.1 V, while the thinner section is 3.3 V. Since both TS were made from the same segment of the ice core, the differences can be explained only by the thicknesses. Most of the grain boundaries are not perpendicular to the TS surface, therefore, the light beam crosses the area which consists of fragments of two or three crystals. In this case, the averaging of output signals occurs. Longitudinal variations of the output signal in a limits of some crystals are caused by the TS surface roughness. Since the thickness of a TS is very small, only one air bubble (Fig. 4b) was detected in both sections with a total length of 225 mm. The mean grain diameter can be obtained by dividing the total length of the TS by the number of grains intersecting the scanning line. The slight deference of the grain numbers in analyzed sections is due to irregular shape and size distribution of ice crystals within the ice core segment.

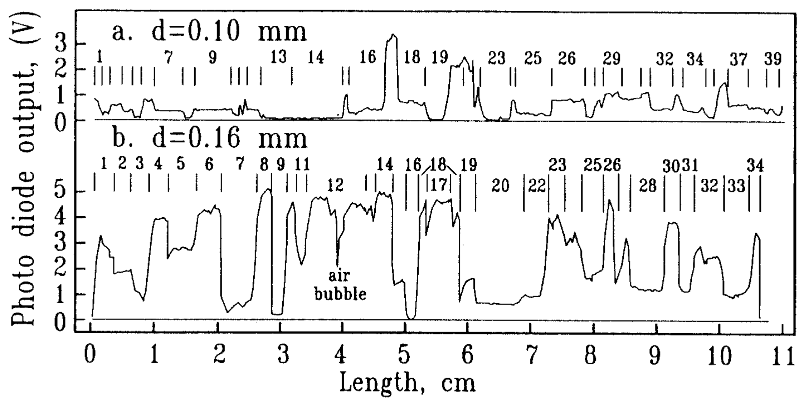

Fig. 4. Intensity of polarized light passing through the thin section-I and analyzer; numbers correspond to the ice crystals visually detected in specimen between cross polaroids. Mizuho Station (Antarctica) ice core, depth 309 m.

3.4. C-axis orientation

It is challenging to use a ICAS for continuous *C*-axis orientation measurements. There are two types of automatic ice fabric analyzers: X-ray Laue method (MORI *et al.*, 1985) and image analysis of thin sections (EICKEN and LANGE, 1992). Both methods used a previously fabricated thin section. Further development of the ICAS will allow us to combine both operations: continuous TS preparation and measurements of optical characteristics of ice crystals. As an option, the image-processing techniques can be involved for continuous ice core analysis.

To check the possibility of the automation of the *C*-axis measurements, the TS-II (Fig. 4b) was scanned thirteen times along the same trace with various incident angles of the laser beam. The profiles similar to those shown in Fig. 4b were obtained. In this way, each crystal was subjected to angular scanning. Using an average output signal along each crystal, the angular dependence was obtained. Results of TS-II scanning are shown in Fig. 5 without correction for light reflection. There are three types of this relationship: a-symmetrical, b-left shifted, and c-right shifted.

Based on the explanation of the polarization effect of the ice crystals by Hobbs, the symmetrical type of relationship occurs when the *C*-axis of the ice crystal is in the plane inclined to the polarization plane by 45° (HOBBS, 1974). Left- and right-shifted curves occur when the angle between projection of the *C*-axis on TS plane and plane of light polarization is defers of from the 45°. Maximal transparency arises when the optic axis is in a plane of the TS (curve 14, Fig. 5). The minimal will occur when the axis is parallel to the TS plane and parallel to the polarization plane (curve 16, Fig. 5a). The *C*-axis of the rest of crystals is inclined to the TS plane. The experimental results shown that within an angle of 180°, each crystal has a particular angle of the maximum transparency.

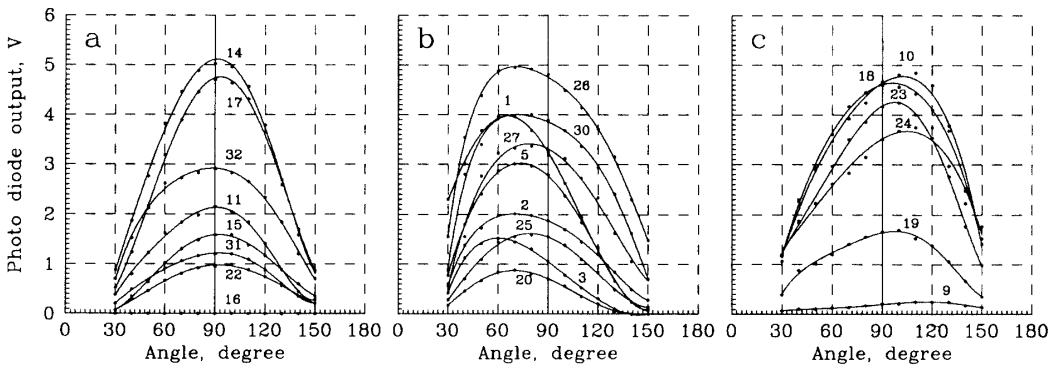

Fig. 5. Intensity of polarized light passing through an ice crystal as a function of the incidence angle; numbers correspond to crystals in Fig. 4.

4. Conclusions

Experiments have demonstrated the opportunity for development of ICAS which is capable of conducting multiple, continuous analyses of an ice cores. The apparatus allows the use of different processing tools and sensors for the multi-task studies of segments of an ice core. The major advantage of the thin section analysis is the small (3 to 5% of ice core volume) ice core waste. It has been demonstrated that a continuous thin section can be used for ECM and optical (density, structure, texture and fabric) ice core investigations.

To improve the capability of ICAS, the following experimental and theoretical investigations should be conducted:

1) correlation between surface potential and ion composition of an ice core;

2) correlation between ice core density and parameters of air inclusions;

3) calculation of relationship between reflection coefficient of polarized light passes through thin section and incident angle;

4) comparison of results of the ice crystal optic axis measurements by conventional and laser scanning method;

5) effect of micro cracks and microparticles on electrical and optical parameters of ice cores.

Acknowledgments

The authors thankful to J. SCHWANDER for many valuable suggestions. This work was supported by the Russian Academy of Sciences, the Japanese Society for the Promotion of Science, the National Institute of Polar Research (Japan), the Swedish Natural Research Council, and the United States National Science Foundation (PICO). Authors are grateful to the Institute of Marine Science, of the University of Alaska Fairbanks for assistance with the technical editing and preparation of this paper.

References

BARKOV, N. I. and LIPENKOV, V. Ya. (1984): Numerical characteristics of ice down to a depth of 1400 m in the region of Vostok Station, Antarctica. Mater. Glaciol. Issled., **51**, 178–186.

BUTKOVICH, T. R. (1953): Density of single crystals of ice from a temperate glacier. U. S. Army SIPRE Research Report 7.

BENSON, C. S. (1959): Physical investigations on the snow and firn of northwest Greenland, 1952, 1953, 1954. U.S. Army SIPRE Research Report 26.

DANSGAARD, W., CLAUSEN, H. B., GUNDESTRUP, N., JOHNSEN, S. J. and RYGNER, C. (1985): Dating and climatic interpretation of two deep Greenland ice cores. Greenland Ice Core: Geophysics, Geochemistry, and the Environment, ed. by C. C. LANGWAY, Jr. *et al.* Washington, D.C., Am. Geophys. Union, 71–76 (Geophysical Monograph 33).

EICKEN, H. and LANGE, M. A. (1991): Image analysis of sea-ice thin sections: a step towards automated texture classification. Ann. Glaciol., **15**, 204-209.

GOW, A. J. (1963): The inner structure of the Ross Ice Shelf at Little America V, Antarctica, as revealed by deep core drilling. Assemblee Generale de Berkeley, Commission des Neiges et des Glaces. Gentbrugge, Association Internationale d'Hydrologie Scientifique, 272–284 (Publication No. 61).

GOW, A. J. and WILLIAMSON, T. (1975): Gas inclusions in the antarctic ice sheet and their significance. CRREL Res. Rep., **339**, 18 p.

HAMMER, C. U. (1980): Acidity of polar ice cores in relation to absolute dating, past volcanism, and radio-echoes. J. Glaciol., **25**, 359–372.

HAMMER, C. U. (1983): Initial direct current in the buildup of space charges and the acidity of ice cores. J. Phys. Chem., **87**, 4099–4103.

HAMMER, C. U., CLAUSEN, H. B., DANSGAARD, W., GUNDESTRUP, N., JOHNSEN, S. and REEH, N. (1978): Dating of Greenland ice cores by flow models, isotopes, volcanic debris, and continental dust. J. Glaciol., **20**, 3–26.

HAMMER C. U., CLAUSEN, H. B. and LANGWAY, C. C., Jr. (1985): The Byrd ice core: Continuous acidity measurements and solid electrical conductivity measurements. Ann. Glaciol., **7**, 214.

HIGASHI, A., NAKAWO, M. and ENOMOTO, E. (1983): The bubble close-of density of ice in Antarctic ice sheets. Mem. Natl Inst. Polar Res., Spec. Issue, **29**, 135–148.

HOBBS, P. V. (1974): Ice Physics. Oxford. Clarendon Press, 837 p.

LANE, J. W. (1975): Optical properties of salt ice. J. Glaciol., **15**, 363–372.

LANGWAY, C. C., Jr. (1958): Bubble pressure in Greenland glacier ice. Symposium de Chamonix 16–24, Sept. 1958. Physique du Mouvement de la Glace. Gentbrugge, Association Internationale d'Hydrologie Scientifique, 336–349 (Publication No. 47).

MORI, Y., HONDOH, T. and HIGASHI, A. (1985): Development of an automatic ice fabric analyzer. Ann. Glaciol., **6**, 281–283.

NAKAWO, M. and NARITA, H. (1985): Density profile of a 413.5 m deep fresh core recovered at Mizuho Station, East Antarctica. Mem. Natl Inst. Polar Res., Spec. Issue, **39**, 141–156.

NARITA, H. and NAKAWO, M. (1985): Structure of 413.5-m deep ice core obtained at Mizuho Station, Antarctica. Mem. Natl Inst. Polar Res., Spec. Issue, **39**, 157–164.

SCHWANDER, J., NEFTEL, A., OESCHGER, H. and STAUFFER, B. (1983): Measurement of direct current conductivity on ice samples for climatological applications. J. Phys. Chem., **87**, 4111–4114.

SHOJI, H. and LANGWAY, C. C., Jr. (1983): Volume relaxation of air inclusions in fresh ice core. J. Phys. Chem., **87**, 4111–4114.

SHOJI, H. and LANGWAY, C. C., Jr. (1989): Physical Property Reference Horizons. Report of the Dahlem Workshop on the Environmental Record in Glaciers and Ice Sheets. Berlin 1988. New York, J. Wiley, 453 p.

SHUMSKII, P. A. (1955): Principles of Structural Glaciology (translated 1964). New York, N.Y. Dover Publ.

STAUFFER, B., BURKHALTER, J. and SIGG, A. (1989): New methods in ice core processing. Ice Core Drilling; Proceedings of the Third International Workshop on Ice Drilling Technology, Grenoble, France, Oct. 10–14, 1988, ed. by C. RADO And D. BEAUDOING. Grenoble, Centre National de la Recherche Scientifique, Laboratoire de Glaciologie et Geophysique de l'Environment, 151–157.

ZAGORODNOV, V. and ARKHIPOV, S. (1990): Studies of structure, composition and temperature regime of sheet glaciers of Svalbard and Severnaya Zemlya: Methods and outcomes. Bull. Glacier Res., **8**, 19–28.

ZAGORODNOV, V. S., HEINTZENBERG, J., WATANABE, O. and FUJII, Y. (1991): Automated measurements of crystal dimensions and concentration of inclusions in ice cores: Methods and firs results. Cold Reg. Sci. Technol., **19**, 327–333.

TAYLOR, K., ALLEY, R., FIACCO, J., GROOTES, P., LAMOREY, G., MAYEWSKI, P. and SPENCER, M. J., (1992): Ice core dating and chemistry by direct-current electrical conductivity. J. Glaciol., **38**, 325–332.

(Received April 20, 1993; Revised manuscript received January 24, 1994)